Numerical Study on the Underground Coal Gasification for Inclined Seams

Lanhe Yang
College of Resources and Geosciences, China University of Mining and Technology, Xuzhou, Jiangsu Province, 221008, China

DOI 10.1002/aic.10554
Published online July 22, 2005 in Wiley InterScience (www.interscience.wiley.com).

According to the characteristics for combustion and gasification reactions occurring in the gasification gallery, the mathematical functional relationship between the chemical reaction rate and every influencing factor is studied. The dynamic nonlinear coupling mathematical models on underground coal gasification of inclined seams are established. The determination methods of major model parameters are introduced. Additionally, the control volume method is adopted to find the numerical solution to the mathematical models. The patterns of development and variation for temperature field, concentration field and pressure field in gasification panel are studied. On the basis of the model test, calculation results are analyzed. From the distribution of temperature field, its calculation value is a little higher than the experimental one, with the relative error of every measuring point virtually within 17%. Research shows that, the experiment value of gas heat value and calculated value take on a good conformity; due to the influence of temperature, in the high temperature zone, the change gradient of the experiment value for concentration field of gas compositions is greater than that of the calculation value. The simulated results indicate that the relative error of the pressure field calculation is 4.13%–12.69% and 8.25%–17.47%, respectively, 7 h and 45 h after the ignition. The drop rate for the fluid pressure is 6.01% and 10.91%, respectively. Research shows that the simulated values conform with experimental values comparatively well, which demonstrates that the numerical simulation on the "three fields" in underground coal gasification is correct. *AIChE J,* 51: 3059–3071, 2005
Keywords: underground coal gasification, mathematical models, temperature field, concentration field, pressure field

Introduction

Field test and laboratory model test verify that the ways of the underground coal gasification is closely related to the occurrences of coal seams. It is easy for the channel gasification to be formed in the gently-inclined coal seams during the underground gasification, while in the steep coal seams, the percolation-patterned gasification is in a primary position.[1] Research shows that in the underground gasification of inclined coal seams, the heat institution and fluid mechanics institution of gasification process are ever-changing. Its thermal conditions and dynamics conditions fall between those of gently-inclined coal seams gasification and those of steep coal seams gasification.[1,2] With the enlargement of the channel diameter, the podzolization of the wall plane for the channel produces gradually, which, in turn, affects the temperature field needed for keeping the normal gas production, leads to the beginning of the combustion–gasification effect weakening for coal seams, and worsens the gasification conditions gradually. However, as the process of gasification occurs, the effect of high temperature and gravitation cause the coal seams on the roof of the channel to continually inbreak. This leads to the gradual

Correspondence concerning this article should be addressed to L. Yang at Lhyang2053@sina.com.

change from free gasification channel to percolation-patterned porous loose channel. Thus, the specific surface area for the reaction between gas and solid carbon increases, improving the gas production conditions.[1–3]

For the development and exploration of the underground coal gasification technique, experiment certainly is an important means, but, recently, people have tended to adopt the method of the combination of experiment and mathematical models. Because the underground coal gasification process is rather complicated, it is comparatively difficult to establish and solve its mathematical models. In spite of those, a number of studies have been made by many scholars home and abroad.[4–13] At one time, a large amount of experimental and theoretical research on the "three fields (temperature field, concentration field and pressure field)" was carried out in countries such as the Former Soviet Union, the United States, China, Germany and France, resulting in great progress.[14–20] While their research results are confined to the general analysis method, experimental method or comparatively simple 1-D, 2-D steady or unsteady-numerical simulation. The dynamic coupling mathematical models on the underground gasification of the inclined coal seams are established in this paper. What's more, the numerical analysis is made. The calculation results are checked against the model test.

The Chemical Reactions in the Underground Coal Gasification Process

During the underground coal gasification, the following seven kinds of chemical reactions mainly take place in the gasification channel

$$(1)\ \mathrm{C} + \mathrm{O_2} \xrightarrow{R_1} \mathrm{CO_2} \quad \Delta H_1 = +393.8\ \mathrm{MJ/kmol}$$

$$(2)\ \mathrm{C} + \mathrm{CO_2} \xrightarrow{R_2} 2\mathrm{CO} \quad \Delta H_2 = -162.4\ \mathrm{MJ/kmol}$$

$$(3)\ \mathrm{C} + \mathrm{H_2O} \xrightarrow{R_3} \mathrm{CO} + \mathrm{H_2} \quad \Delta H_3 = -131.4\ \mathrm{MJ/kmol}$$

$$(4)\ \mathrm{C} + 2\mathrm{H_2} \xrightarrow{R_4} \mathrm{CH_4} \quad \Delta H_4 = +74.9\ \mathrm{MJ/kmol}$$

$$(5)\ \mathrm{CO} + \frac{1}{2}\mathrm{O_2} \xrightarrow{R_5} \mathrm{CO_2} \quad \Delta H_5 = +285.1\ \mathrm{MJ/kmol}$$

$$(6)\ \mathrm{H_2} + \frac{1}{2}\mathrm{O_2} \xrightarrow{R_6} \mathrm{H_2O} \quad \Delta H_6 = +242.0\ \mathrm{MJ/kmol}$$

$$(7)\ \mathrm{CO} + \mathrm{H_2O} \xrightarrow{R_7} \mathrm{CO_2} + \mathrm{H_2} \quad \Delta H_7 = +41.0\ \mathrm{MJ/kmol}$$

The above reactions are the main basis for the conservation of mass equation of the chemical reactions. (1), (2), (3) and (4) reactions take place on the wall plane of the coal seams, while (5), (6) and (7) reactions occur at the gaseous stage. During the underground gasification, due to the high temperature, the coal seams crack. The combustion reactions must cause the O_2 to diffuse to the surface of the carbon where reaction has not yet occurred. Theory proves that, under the underground combustion and gasification condition, the diffusion mass transfer of the gas passing through the surface grieshoch is the major factor controlling the carbon reaction rate. The gasification reaction is controlled by the diffusion process. The diffusion rate of the mole number for gas compositions equals the dynamic reaction rate of coal surface.[21] On the basis of the above, we can obtain every chemical reaction rate R_j. The influence of temperature on the reaction rate is mainly reflected on the constant of reaction rate, the value of K.

According to literature,[21] the Arrhenius formula is

$$K = A_c \exp(-\Delta E/RT) \tag{1}$$

According to the Eq. 1 and the research findings[22] of V. Fredersdorff and M. A. Elliott, we can obtain

$$R_1 = A_c \exp(-\Delta E_1/RT)\, P_{\mathrm{O_2}} \tag{2}$$

$$R_2 = A_c \exp(a/T - bT)\, P_{\mathrm{CO_2}} \tag{3}$$

$$R_3 = A_c \exp(-\Delta E_3/RT)\left(P_{\mathrm{H_2O}} - \frac{1}{K_f} P_{\mathrm{CO}} P_{\mathrm{H_2}}\right) \tag{4}$$

where

$$K_f = \exp(-\Delta G/RT) \tag{5}$$

where

$$R_4 = A_c \exp(-\Delta E_4/RT)\left(P_{\mathrm{H_2}}^2 - \frac{1}{K_f} P_{\mathrm{CH_4}}\right) \tag{6}$$

$$R_5 = A_c \exp(-\Delta E_5/RT)\, P_{\mathrm{CO}} \tag{7}$$

$$R_6 = A_c \exp(-\Delta E_6/RT)\, P_{\mathrm{H_2}} \tag{8}$$

$$R_7 = \frac{\left(\frac{K_1}{K_{-1}}\right)^{1/2} P_{\mathrm{H_2}}^{1/2} (K_2 K_3 P_{\mathrm{H_2}} P_{\mathrm{CO_2}} - K_{-2} K_{-3} P_{\mathrm{CO}} P_{\mathrm{H_2O}})}{K_{-2} P_{\mathrm{CO}} + K_3 P_{\mathrm{H_2}}} \tag{9}$$

where

$$K_1 = a_1 T^{-b_1} \exp(-\Delta E_1/RT) \tag{10}$$

$$K_2 = a_2 T^{-b_2} \exp(-\Delta E_2/RT) \tag{11}$$

$$K_{-2} = a_{-2} \exp(-\Delta E_2/RT) \tag{12}$$

$$K_{-3} = a_{-3} \exp(-\Delta E_3/RT) \tag{13}$$

$$K_3 = a_3 \exp(-\Delta E_3/RT) \tag{14}$$

$$K_{-1} = \frac{a_{-1}}{T} \tag{15}$$

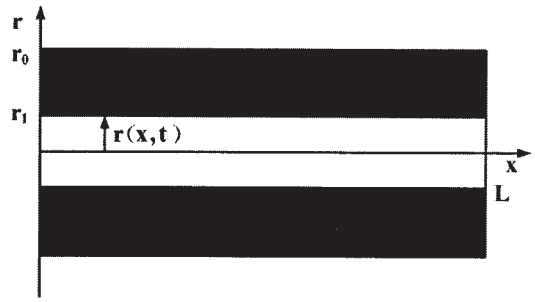

Figure 1. Model gasifier.

where K_j is the equilibrium constant of chemical reaction j, K_f is the equilibrium constant expressed in terms of the partial fugacity of every composition; ΔE_j is the activation energy of chemical reaction j, R is universal gas constant; ΔG is the free enthalpy of standard formation when the temperature stands at T, P_i is the partial pressure of composition i in the mixed gas.

Coupled Mathematical Models

Assumed conditions

In the course of the combustion and gasification for the coal seams, various complex physical and chemical reactions occur in the gasifier. Meanwhile, there are energy and mass transfer between gas phase and solid phase. In this paper, in order to simplify the calculation, the following assumptions are made:

(1) The gasifier itself is in a stable working state. Major physical and thermodynamic parameters, such as coefficient of heat conductivity, specific heat and coefficient of heat exchange do not vary with time,[23]

(2) Thermal diffusion and pressure diffusion will be ignored,[24]

(3) The effect of thermal resistance will be ignored;

(4) The change in the mass of gas current in the oxidation zone due to the chemical reactions will be ignored;[25]

(5) For the inclined coal seams, since its thickness is much smaller than its slant height and strike length, temperature conduction and the movement of the mixed gas in the coal layer can be simplified into a 2-D problem (Figure 1).

In the multicomponent gas, take a control body with an encompassed area of F, in which every component occupies the same area. Tracing the changes of the control body with the movement gives the changes of various parameters with the time. If a certain characteristic variable of the control body is φ, the total of the φ in the control body will be ϕ. Then, in the cylinder-coordinate system, we have

$$\phi(t) = \int\int_F \varphi(x, r, t)dF \tag{16}$$

Conservation equation of the compositions

In the process of underground coal gasification, there are mainly seven kinds of compositions in the product gas, in the paper, only the balance of these seven kinds of compositions is taken into consideration, which are, in turn, O_2 (1), CO_2 (2), CO (3), H_2O (4), H_2 (5), CH_4 (6) and N_2 (7). According to the document,[26] considering axial flow and axial and radial diffusion, we can obtain the conservation equation of the compositions

$$\frac{\partial y_i}{\partial t} + \frac{\partial y_i}{\partial x}(uy_i) = \frac{\partial}{\partial x}\left(D\frac{\partial y_i}{\partial x}\right) + \frac{\partial}{\partial r}\left(D\frac{\partial y_i}{\partial r}\right) + D\frac{1}{r}\frac{\partial y_i}{\partial r} + S_i \quad i = 1, 2, \ldots, 7 \tag{17}$$

where y_i is the mole fraction of the composition i (O_2, CO_2, CO, H_2O, H_2, CH_4, N_2); u is only taking the gas flowing speed along the axial direction into consideration; D is regarding the diffusion rate of every composition along the axial and radial direction the same, therefore, $D_{eff,i} = D$; S_i is the generating rate of the composition i in the chemical reaction.

From the earlier seven kinds of chemical reaction equations, we can obtain

$$S_1 = -R_5 - R_6 \tag{18}$$

$$S_2 = 2R_5 \tag{19}$$

$$S_3 = -2R_5 \tag{20}$$

$$S_4 = 2R_6 \tag{21}$$

$$S_5 = -2R_6 \tag{22}$$

$$S_6 = S_7 = 0 \tag{23}$$

Initial conditions and boundary conditions:

(1) Boundary Conditions

Measuring and analyzing the gas compositions at the inlet of the gasification gallery, we can obtain the concentration of gasification agent at the inlet, that is

$$\text{At } x = 0, \quad y_i = y_{i0}, \quad 0 \le r \le r_1, \quad t > 0 \tag{24}$$

where y_{i0} is the mole fraction of gasification agent at the inlet of gallery.

Because there is little change in the gradient of concentration for every gas composition at the outlet of gasification gallery, the gradient of concentration for the gas composition i at the outlet can be regarded as zero, that is

$$\text{At } x = L, \quad \frac{\partial y_i}{\partial x} = 0, \quad 0 \le r \le r_1, \quad t > 0 \tag{25}$$

where L is the length of gallery, the subscript "0" of the variable denotes the known value of parameter.

At $r = r_1$, that is, at the boundary of the wall plane for the coal seams, the boundary conditions are

$$D\frac{\partial y_1}{\partial r} + \frac{r_1}{2}R_1 = 0 \tag{26}$$

$$D\frac{\partial y_2}{\partial r} + \frac{r_1}{2}(-R_1 + R_2 - R_7) = 0 \tag{27}$$

$$D\frac{\partial y_3}{\partial r}+\frac{r_1}{2}(-2R_2-R_3+R_7)=0 \tag{28}$$

$$D\frac{\partial y_4}{\partial r}+\frac{r_1}{2}(R_3+R_7)=0 \tag{29}$$

$$D\frac{\partial y_5}{\partial r}+\frac{r_1}{2}(R_4+R_3-R_7)=0 \tag{30}$$

$$D\frac{\partial y_6}{\partial r}+\frac{r_1}{2}\left(\frac{R_4}{2}\right)=0 \tag{31}$$

$$D\frac{\partial y_7}{\partial r}=0 \tag{32}$$

(2) Initial Conditions

Before the gasification, the content for the composition i in the gasification agent is known, that is

$$t\le 0,\quad y_i=y_{i0},\quad 0\le r\le r_1,\quad 0\le x\le L \tag{33}$$

Conservation equations of energy solid phase

Considering the interior heat conduction gives the temperature field equation of coal seams[26,27]

$$\rho_S C_S\frac{\partial T_S}{\partial t}=\frac{\partial}{\partial x}\left(\lambda_S\frac{\partial T_S}{\partial x}\right)+\frac{\partial}{\partial r}\left(\lambda_S\frac{\partial T_S}{\partial r}\right)+\frac{1}{r}\lambda_S\frac{\partial T_S}{\partial r}-Q_S \tag{34}$$

where T_S is the temperature of solid phase, C_S is the specific heat of solid phase, Q_S is the heat losses of solid phase, λ_S is the coefficient of heat conductivity for the solid phase, ρ_S is the density of solid phase.

Equation 34 must meet the following boundary conditions and initial conditions: According to the measurement results for the temperature field in the gasifier, the temperature of the outer coal seam with a radius of r_0, and temperature at the inlet of gasification gallery can be known. Because there is little change in the gradient of temperature for coal seams at the outlet of gasification gallery, it can be regarded as zero, that is

$$\text{At } r=r_0,\quad T_S=T_{S\infty},\quad 0\le x\le L,\quad t>0 \tag{35}$$

$$\text{At } x=L,\quad \frac{\partial T_S}{\partial x}=0,\quad r_1<r<r_0,\quad t>0 \tag{36}$$

$$\text{At } x=0,\quad T_S=T_0,\quad r_1<r<r_0,\quad t>0 \tag{37}$$

where $T_{S\infty}$ is the temperature of the outer coal seam with a radius of r_0, assumed to be a constant.

At the gas-solid interface where $r=r_1$, because there is heat convection between gas and solid and heat and mass transfer, the following conditions should be met

$$\lambda_S\frac{\partial T_S}{\partial t}=\alpha(T_S-T_g)-\sum_{i,j=1}^{7}m_i\Delta H_j+RHT \tag{38}$$

where m_i is the mass flowing quantity of the composition i, ΔH_j is the reaction heat of the chemical reaction j, α is the coefficient of heat convection, T_g is the temperature of gas phase, RHT is the quantity of heat exchange by radiation,[26] that is

$$RHT=F_1\sigma\varepsilon_q(T_S^4-T_g^4) \tag{39}$$

where σ is Stefan-Baltzmann constant, ε_q is the coefficient of heat radiation, F_1 is the area of heat radiation,[26]

$$F_1=2\pi\int_0^L r(x,t)dx \tag{40}$$

Initial conditions

According to the measured results for the temperature of coal seams before ignition, the temperature for the solid phase can be known when

$$t=0,\quad T_S=T_{S0},\quad 0\le z\le L,\quad 0\le r\le r_1$$

where T_{S0} is the known temperature of the solid phase.

Gas phase

According to the documents,[28,29] we can obtain the conservation equation of energy for gas phase

$$\nabla\cdot\left(\sum_{i,j=1}^{7}\gamma_j H_i\cdot\nabla m_i\right)+\nabla\cdot(\lambda_g\cdot\nabla T_g)+SH-Q_g=\rho_g C_{gi}\frac{\partial T_g}{\partial t}+u\rho_g C_{gi}\frac{\partial T_g}{\partial x} \tag{41}$$

where γ_j is the coefficient of weighing and measuring for the chemical reaction j, H_i is the enthalpy of formation for the gas composition i, SH is the heat of formation for the gas phase, C_{gi} is the specific heat of the composition i for the gas phase, λ_g is the coefficient of heat conductivity for the gas phase, ρ_g is the density of the mixed gas, Q_g is the heat losses of the gas phase where $\gamma_j=\rho_g D$.[21]

Simplifying Equation 41 gives

$$\sum_{i,j=1}^{7}\left[\rho_g m_i(T_g)C_{gi}(T_g)\frac{\partial T_g}{\partial t}-C_{gi}(T_g)\nabla T_g\gamma_j\nabla m_i\right]-\nabla\lambda_g\nabla T_g+\sum_{i=1}^{7}H_i m_i-Q_g=R_5\Delta H_5+R_6\Delta H_6 \tag{42}$$

Boundary conditions

Measuring the gas temperature in the gasification gallery, the gas temperature at the inlet and temperature gradient for the gas at the outlet can be known, that is

$$\text{At } x = 0, \quad T_g = T_{gb}, \quad 0 \le r \le r_1, \quad t > 0 \tag{43}$$

$$\text{At } x = L, \quad \frac{\partial T_g}{\partial x} = 0, \quad 0 \le r \le r_1, \quad t > 0 \tag{44}$$

Wall plane boundary

In the proximity of wall plane, there is similarly heat convection and heat radiation between heat current and wall plane, whose boundary conditions can be shown as

$$\text{At } r = r_1, \quad \lambda_g \frac{\partial T_g}{\partial r} = \alpha(T_S - T_g) + RHT, \quad 0 \le x \le L, \quad t > 0 \tag{45}$$

$$\text{At } r = 0, \quad T_g = T_{gp}, \quad 0 \le x \le L, \quad t > 0 \tag{46}$$

Initial conditions

According to the measured results for the gas temperature in the gasification gallery before ignition, the initial temperature of the gas can be known, that is, when

$$t = 0, \quad T_g = T_{g0}, \quad 0 \le x \le L, \quad 0 \le r \le r_1 \tag{47}$$

where T_{g0} is the initial temperature of the gas.

Equation of the gas phase movement

As stated earlier, in the process of the underground coal gasification, the flow of the mixed fluid in the gallery can be regarded as the seepage movement of the gas in the porous media.[1] Thus, in so doing, the equation of the gas movement can be obtained

$$\frac{\partial P_g}{\partial t} = a_c \left[\nabla \cdot \left(\frac{1}{a_0 + b_0 u} \nabla P_g \right) + W_g \right] \tag{48}$$

where P_g is the fluid pressure; a_c is the coefficient of conduction pressure; W_g is the source-sink item, depending on the generating rate of the gas phase; parameters a_0 and b_0 are determined by the following two formulas, respectively

$$a_0 = \nu / g \bar{e} r_g, \quad b_0 = \beta d / g \bar{n} \bar{e} r_g$$

where ν is the coefficient of movement viscosity, g is the gravitational acceleration, $\bar{e}$ is the permeability, r_g is the weight degree, β is the coefficient of geometrical shape for the media particles, d is the average compromising particle size, $\bar{n}$ is the porosity.

Gas state equation

In the process of underground coal gasification, the gas state equation can be shown as follows

$$P_g = CRT_g \tag{49}$$

where C is overall mole concentration of the gas.

Unified form of the conservation and movement equations

The earlier conservation and movement equations can be written into a unified form, that is

$$\frac{\partial(\rho\phi)}{\partial t} + \text{div}(\rho u \phi - \Gamma_\phi \text{grad}\ \phi) = S_\phi \tag{50}$$

where ϕ is the dependent variable; Γ_ϕ and S_ϕ indicate the coefficient of exchange and source corresponding to ϕ, respectively. The equation can be regarded as being made up of four items, which are transient item, convection item, diffusion item and source item, in turn.

Numerical Calculation

In view of the nonlinearness for the earlier control equations and the strong coupling among equations, so it is difficult to solve them through analysis method, making us have no choice but to employ the numerical solution. In this article, the control volume method[26,30] is adopted, which is a discretization method belonging to the finite difference method in the form, but being not fundamentally different from finite element method in methodology. The method aims at the integral equilibrium in the control volume, uses knot to represent control volume. The discretization of the domain to be solved usually includes two kinds, namely, even grid and uneven grid. On the basis of the characteristics of the problem to be addressed in the paper, every variable is the function of time for its spatial distribution. Hence, in the process of solution, the grid will be divided according to the even grid.

The discretization of Eq. 50 depends on the following two basic assumptions:

(1) The function value is evenly distributed in each grid, that is, the function value on the node of the grid represents its value everywhere within the grid, or we can say, the size of the grid determines the spatial resolution ratio of the function.

(2) The function value is evenly distributed on each interface for each grid, that is, the function value at an arbitrary point of the boundary of the grid can represent the function value at that boundary. Usually, the crossover point between the ligature of the two neighboring points on both sides of the boundary for a certain grid and the boundary is selected as the representative point of that boundary.

Integrate Eq. 50 on the grid centered around point P, we can obtain the commonly-used form of the difference equation

$$\frac{\partial}{\partial t}(\rho\phi F_\phi)_P + \sum_{\substack{e,w \\ n,s}} [(\rho u \phi - \Gamma_\phi \text{grad}\ \phi) \cdot \mathbf{A}] = (S_\phi F_\phi)_P \tag{51}$$

where F_ϕ indicates the area of the grid, varying with time, under this circumstance, u takes the velocity of the fluid relative to the moving boundary of the grid. The absolute value of A indicates the length of a certain interface for the grid, whose direction is that of the outer normal for the interface, Σ indicates taking a sum of the four boundaries for the grid.

Discretization of the transient item

The expression of the discretization for the transient item is

$$\int_{t-\Delta t}^{t} \frac{\partial}{\partial t}(\rho\phi F_\phi)_P dt = (\rho\phi F_\phi)_P - (\rho\phi F_\phi)_{P^0} \tag{52}$$

where superscript "0" denotes the state of the point P at the previous time, $t - \Delta t$; Δt is time step size.

Discretization of the source item

Assuming adopting the fully implicit form when making the integration of the source item in Eq. 51 relative to time, that is

$$\int_{t-\Delta t}^{t} (S_\phi F_\phi)_P dt = (S_\phi F_\phi)_P \Delta t \tag{53}$$

If the source item is a constant one, its discretized expression will be the form of Eq. 53.

If the source item is the function of the variable ϕ, generally the linearization method will be adopted to further discretize the source item, that is, write the source item S_ϕ in the general form of the differential Eq. 50 personally as

$$S_\phi = S_C + S_P\phi \tag{54}$$

where S_C and S_P are constants relative to ϕ, actually they can either be a real constant or the function of the previous iterative value ϕ^* for the variable ϕ.

Discretization of the total flux item

The item in the Σ of the Eq. 51 combines the influence of the convective flux, and the diffusion flux, known as the total flux item. Write the total flux as $\mathbf{J}$

$$\mathbf{J} = (\rho u\phi - \Gamma_\phi \text{grad}\ \phi) \tag{55}$$

In view of the similarity for the principles and treatment method in which the total flux item is discretized at each interface, now we will take the calculation of the total flux for an arbitrary grid interface (for example, e plane) as an example (Figure 2), so as to illustrate the discretization method of the total flux item.

At the e plane of the grid P, the general flux item is

$$\mathbf{J}_e = \mathbf{J}\cdot\mathbf{A}_e/\mathbf{A}_e = \left[(\rho u)\phi_e - \Gamma_e\left(\frac{d\phi}{dx}\right)_e\right] \tag{56}$$

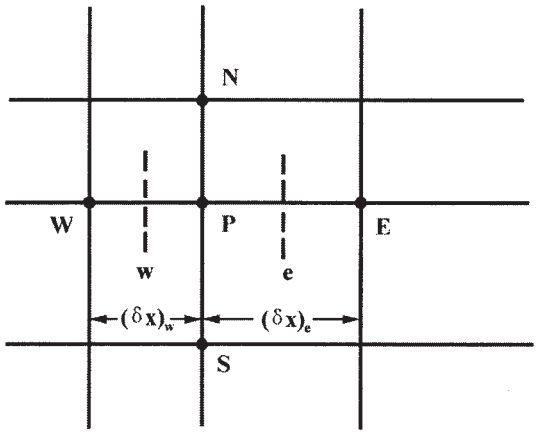

Figure 2. Grid points and grid interface.

For the convenience of the writing, the discretized expression of the general flux item at the e plane can be written as

$$\mathbf{A}_e\mathbf{J}_e = C_e\phi_e - D_e(\phi_E - \phi_P) \tag{57}$$

where

$$C_e = (\rho uA)_e \tag{58}$$

$$D_e = \Gamma_e A_e/(\delta x)_e \tag{59}$$

C_e indicates the convection (or flowing) intensity at the e plane, whose sign is determined by the direction of u, D_e indicates the diffusion intensity at the e plane, always to be positive.

Normally, the exchange coefficient Γ_e at the interface takes the arithmetic average of the exchange coefficient for two neighboring grid points. In the even grid system

$$\Gamma_e = \frac{1}{2}(\Gamma_P + \Gamma_E) \tag{60}$$

Discretized equation

On the basis of the numerical model established earlier for the 2-D problem, the author developed the generally-used computer program used to solve for the mathematical models on the 2-D nonlinear dynamic reaction flow in the underground coal gasification, and realized the calculation of the models in this article. The general form and its corresponding coefficients for the discretized (finite difference) equations of the control differential, Eq. 50, in 2-D unsteady problem, are as follows

$$a_P\phi_P = a_E\phi_E + a_W\phi_W + a_N\phi_N + a_S\phi_S + b_C \tag{61}$$

where

$$\left.\begin{aligned} a_E &= D_e A(|\overline{P_e}|) + [[-C_e, 0]] \\ a_W &= D_w A(|\overline{P_w}|) + [[C_w, 0]] \\ a_N &= D_n A(|\overline{P_n}|) + [[-C_n, 0]] \\ a_S &= D_s A(|\overline{P_s}|) + [[C_s, 0]] \\ a_{P^0} &= \rho_{P^0} F_\phi / \Delta t \\ b_C &= S_C F_\phi + a_{P^0} \phi_{P^0} \\ a_P &= a_E + a_W + a_N + a_S + a_{P^0} - S_P F_\phi \end{aligned}\right\} \quad (62)$$

In the coefficient expressions, a_I indicate coefficients of difference equation corresponding to different grid points ($I = E, W, N, S$); b_C is constant term, ρ_{P^0} is the fluid density of the point P at the previous time, C_k and D_k are the convection intensity and diffusion intensity of the k interface, respectively, P_k is the ratio of the two; their definition expressions are

$$\left.\begin{aligned} C_k &= (\rho u A)_k \\ D_k &= \frac{\Gamma_k A_k}{\delta_k} \\ P_k &= \frac{C_k}{D_k} \end{aligned}\right\} \quad (63)$$

$k = e, w, n, s$ indicates the grid interface between two grid points, A_k is the length of the k interface, δ_k is the distance between two grid points on the vertical k interface.

The distribution of the variable in the control volume takes the power function, so, for different circumstances, the form function $A(|\bar{P}|)$ may be selected various forms, selecting power law form in the article, that is

$$A(|\bar{P}|) = [[0, (1 - 0.1|\bar{P}|)^5]] \quad (64)$$

where $\bar{P}$ is Peclet number, indicating the relative intensity of convection and diffusion; the operator [[ ]] denotes selecting the maximum in the square brackets.

According to the difference equations established, we can obtain the simultaneous algebraic equation set of the control equations. On the basis of this, it is comparatively easier to adopt the separated iterative solution.

Model Parameters

Specific heat of gas phase, C_{gi}

The specific heat of the gas phase mixture normally depends on its thermodynamics state. The relational form for the specific heat used in this article is as follows

$$C_{gi} = \bar{A}_i + \bar{B}_i T^{n1} + \bar{C}_i T^{n2} \quad (65)$$

where $\bar{A}_i$, $\bar{B}_i$, $\bar{C}_i$, $n1$ and $n2$ are coefficients of the expression, which vary with the kinds of substances and are irrelevant to temperature, whose specific values can be referred to in reference 26.

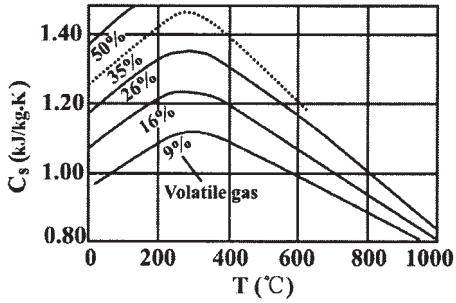

Figure 3. Relation between the specific heat and temperature of coal.

Specific heat of solid phase, C_S

The experimental research shows that the specific heat for solid substances containing carbon is linked to its characteristic composition and temperature, whose relationship is shown in Figure 3. In the process of inversion calculation, C_S will be determined according to the Figure 3.

Coefficient of heat convection, α

Gas-solid phase reactions mainly occur in the pores of solid phase, the heat of the heterogeneous reaction is applied to the solid phase. When the oxidation reaction, the solid-phase transfers heat to gas phase, while reduction, dry and distillation, the gas phase transfers heat to solid phase.

There are heat-transfer by convection and heat-transfer by radiation in the gas-solid heat exchange. When the temperature is high, heat-transfer by radiation will play a major role. Additionally, when the diameter of the particle is comparatively big, the heat conduction of the particle itself has to be taken into consideration. In the gas-solid heat transfer, the temperature of every point is shown in Figure 4. The quantity of heat transfer is calculated as follows[31]

$$Q = \alpha F_S (T_g - T_S) \quad (66)$$

where

$$\alpha = \frac{1}{\dfrac{1}{\alpha_L + \alpha'_S} + \dfrac{1}{\alpha_K + \alpha_S}} \quad (67)$$

$$\alpha_L = \frac{2}{\left(\dfrac{1}{R_r} + \dfrac{1}{R_K}\right) R_K^2} \quad (68)$$

$$\alpha'_S = \varepsilon_S \delta (T_K^3 + T_K^2 T_{K1} + T_K T_{K1}^2 + T_{K1}^3) \quad (69)$$

$$\alpha_K = \frac{N_u \lambda_g}{D_K} \quad (70)$$

$$\alpha_S = \varepsilon_0 \delta_0 (T_{K1}^3 + T_{K1}^2 T_g + T_{K1} T_g^2 + T_g^3) \quad (71)$$

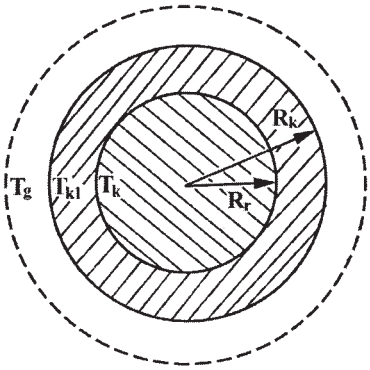

Figure 4. Temperature distribution for gas-solid heat transfer.

$$\varepsilon_0 = \frac{1}{\frac{1}{\varepsilon_S} + \frac{1}{\varepsilon_g} - 1}, \quad \varepsilon_S = 0.7 - 0.8 \tag{72}$$

In the earlier formula, α_L and α'_S are the coefficient of heat convection, and that of heat-exchange by radiation through ash dreg layers, respectively; α_K and α_S are the coefficient of heat convection and that of heat-exchange by radiation through reduced film, respectively; ε_S and ε_g is the radiation rate of solid phase and gas phase, respectively; N_u is Nulet dimensionless number; δ and δ_0 are the thickness of the ash dreg layer and that of the reduced film, respectively; F_S is the specific surface area of the solid particle; D_K is the diameter of the particle; R_r is the radius of the reaction core, R_K is the radius of the particle; T_K is the temperature of reaction core; and T_{K1} is the temperature of the solid particle.

Permeability, $\bar{e}$

Experimental research shows that, under the nonisothermal condition, the permeability of the porous media is a function of temperature.[1,2,29] With the movement of the flame working face, in the process of combustion and gasification, since there are great temperature differences for the coal layers at various sections, great changes will take place in the permeability. Under the nonisothermal condition, the measured results of the permeability for the coal layers media used in the experimental model are shown in Figure 5. The input of this parameter is mainly based on the experimental data shown in Figure 5.

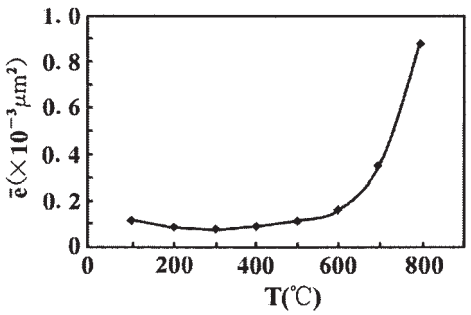

Figure 5. Changing curve of permeability and temperature.

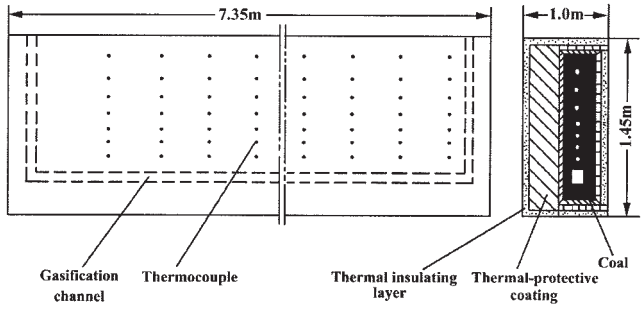

Figure 6. Cutaway view of the gasifier model.

Coefficient of heat conductivity, λ_S

Under the condition of the combustion and gasification for the coal layers, the total coefficient of the heat conductivity for the media also consists of heat conduction and heat radiation, whose expression is as follows[1]

$$\lambda_S = \zeta_1(T) + \zeta_2(T) \tag{73}$$

where $\zeta_1(T)$ is the function of the coefficient of heat conductivity for coal mass; $\zeta_2(T)$ is the function of the coefficient of heat-exchange by radiation among coal chunks.

Other parameters

Other parameters in the mathematical model, such as the coefficient of diffusion, the enthalpy of formation and the coefficient of viscosity, are all functions of temperature under the nonisothermal condition, whose specific calculation method can be referred to in the relevant documents.[32–36]

Because temperature has an important effect on model parameters, in the process of inversion calculation, the values of parameters shall be initially determined, based on the relationship between each parameter and temperature and temperature values at different nodes. Then through positive calculation, we will judge the reasonability of the model parameters selected. If the errors between calculated values and experimented values are within tolerance, the parameters selected are right, otherwise, further adjustments or correction should be made on every parameter till comparatively ideal calculated results have been obtained.

Model Test

The overall size of the model gasifier body is 7.35 m long by 1.45 m high by 1.0 m thickness, consisting of base and lid, as shown in Figure 6. Under the bottom of the gasifier was installed a line of hydraulic jacks, which makes the gasifier rest at any angle. The hearth is so spacious that it can be filled with other materials, which are used to simulate coal seams with different thickness. On the sides of the gasifier there are a number of gas inlets, outlets, and slip casting holes, used to simulate various gasifiers and study different modes of air pumping and gasification channel with different lengths. A circular air (steam) injection pipeline is equipped on the platform in hope for supplying the air (steam) in the same or counter direction and with moving pumping points. The gasifier adopts hydraulic sealing technology. On the upside of the

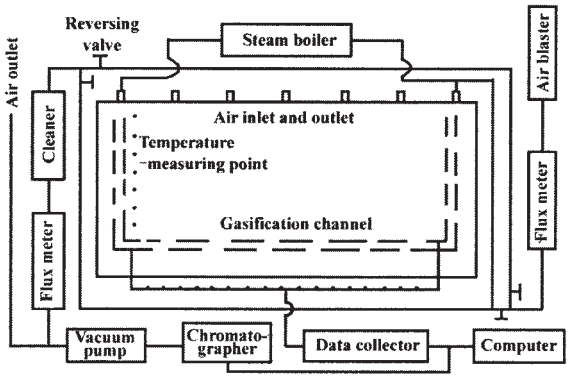

Figure 7. System of model experiment.

gasifier is installed a piece of board pushed by hydraulic push rod, which imposes a certain pressure on the coal seams through the board in the course of gasification, in order to simulate the pressure on the top of the coal seams.

The structure of the gasifier is made up of three layers. The outer one is sealant made of thick steel plate, with the middle one thermal insulating made of vermiculite, the inner one flame retardant coating. The size of simulated coal seams in the gasifier is 6.7 m × 1.3 m × 0.45 m, with a dip angle of about 45°. The type of coal is gas-fat coal. The data of the proximate analysis can be consulted in the document.[1] In the process of coal injection, use as much lump coal as possible, so we can keep the natural state of the coal seams at best. The interstices will be filled with small pieces of coal. Finally, smear the interstices with the mixture of cement and coal powder. The gasification panel is 6.0 m × 1.1 m × 0.42 m. The initial equivalent diameter of the gasification gallery is 80 mm.

The system of the model test is shown in Figure 7. The pipeline system is designed as an armillary circuit. Through the reversal valve, we can pump the air or steam negatively and positively. Coal gas cleaner is mainly to remove the tar from the gas and lower the temperature of the resulting gas. In order to measure the temperature distribution in the gasifier accurately, we deploy the temperature-measuring points intensively. In the gasification panel, 17 rows of temperature-measuring points are buried, with 7 in each row. The number totals

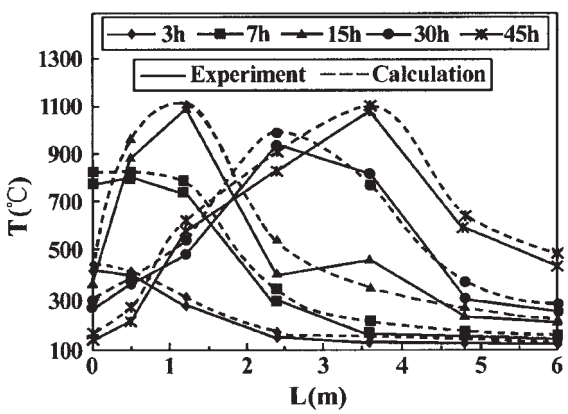

Figure 8. Experiment value and calculation value of the temperature field at various times of gasification.

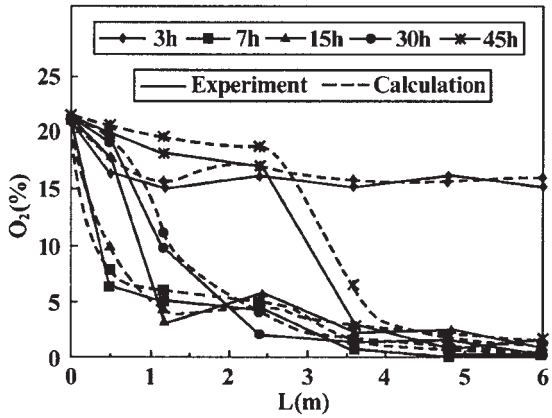

Figure 9. Experiment value and calculation value of the concentration of O_2 at various times of gasification.

119. The temperature-measuring elements adopt the strictly-standardized NiCr-NiSi thermal couples. The automatic data acquisition will be made regularly, and the data will be displayed on the screen of the computer and recorded. The resulting gas will be analyzed with gas-phase chromatographer, which can tell the contents of different compositions. Every bore hole deployed at the sides of gasifier along the direction of gasification gallery also has the monitoring function. In the experiment, the real-time monitor has been made against the pressure and gas compositions in the gasifier, so as to learn the state of changes for the pressure field and concentration field at different places and various times within the gasification gallery.

The operating conditions: the gasification agent, air; the pressure at the inlet, 2550–2600 Pa; the flowing capacity at the inlet, 25–30 m^3/h. The results of the experiment are shown in Figures 8–15.

Analysis

The calculation results of numerical simulation are shown in Figures 8–15. From Figure 8, it can be shown that the calcu-

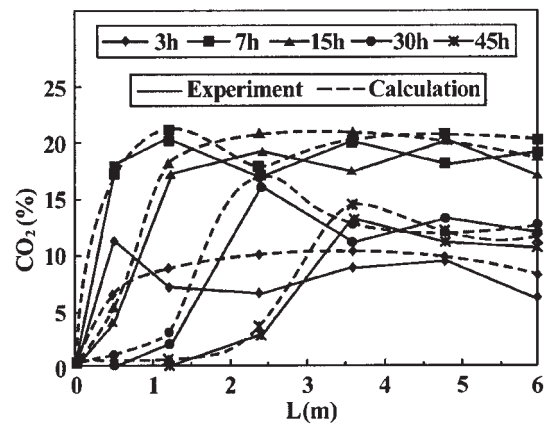

Figure 10. Experiment value and calculation value of the concentration of CO_2 at various times of gasification.

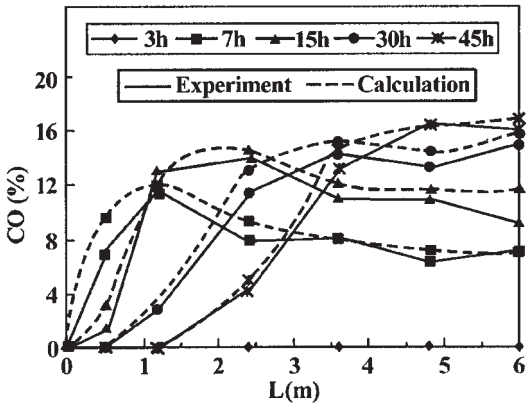

Figure 11. Experiment value and calculation value of the concentration of CO at various times of gasification.

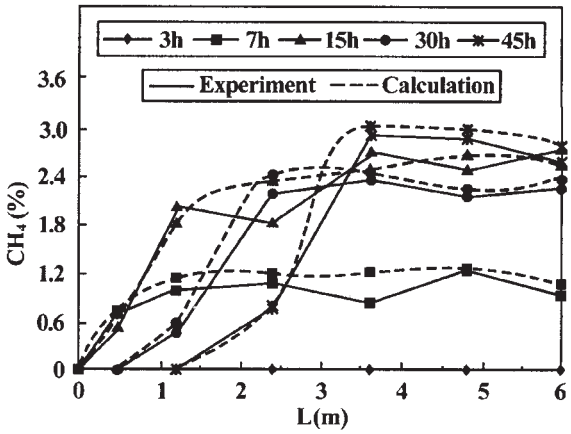

Figure 13. Experiment value and calculation value of the concentration of CH_4 at various times of gasification.

lated values of temperature field virtually conform with the measured ones. Except the measuring points in the combustion zone, where the relative error between the calculated values and measured ones of temperature is rather high (certain points, over 20%), the relative error of other points is no more than 17%, majority of which is within 14%, completely meeting the precision requirement of numerical simulation on the temperature field. Judging from the distribution of temperature field, the calculated values are a bit bigger than the measured ones. The reasons are the following: first of all, the term of heat losses in the mathematical model is determined on such conditions as the calculation formula for the coefficient of heat transfer with the composite structure and fixed setting (temperature, wind velocity). In the process of experiment, natural ventilation or forced ventilation makes the coefficient of heat losses increase, which contributes to the slight drop in the measured temperature. Then, during calculation, the coefficient of heat conductivity for coal seams is not that of body coal but the equivalent coefficient of heat conductivity for coal seams taking the influence of convection and heat radiation into consideration. The coal seams in the model test are piled up selecting various sizes of coal chunks. Though the interstices are filled with pulverized coal, its pores are far bigger than those of the natural ones. Therefore, heat transfer is no longer a single form of heat conduction. With the effect of convection intensifying, the coefficient of apparent heat conduction for the coal seams heightens, which influences the calculation results precision.

Because the reaction rate heightens rapidly with the rise in temperature, which leads to the increase in the reaction conversion rate, as a result, the influence of the temperature causes the calculated values of the concentration for various compositions in gas to be a little bigger than the experimental ones; the change gradient of the composition concentration for experimental value in high-temperature zone is bigger than that of the calculated value (Figures 9–13).

According to Figure 14, with the prolonging of gasification time and the increase in the gasification channel length, the heating value of gas increases gradually, and there is virtually no fluctuation for it. Therefore, the experimental values and the calculated ones take on a good conformity. However, beyond the reduction zone, the extent of increase for the heating value decreases. The influence of temperature field on the heating value of gas is remarkable. 7 h after the ignition, in spite of the

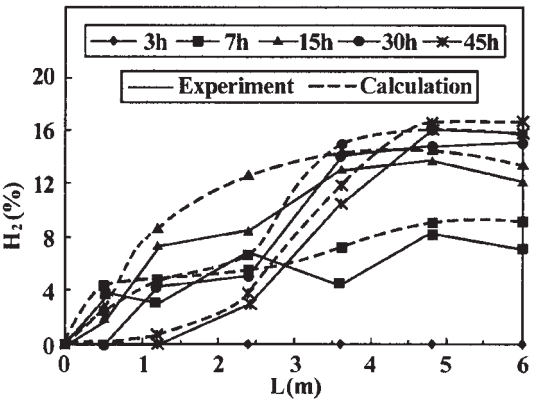

Figure 12. Experiment value and calculation value of the concentration of H_2 at various times of gasification.

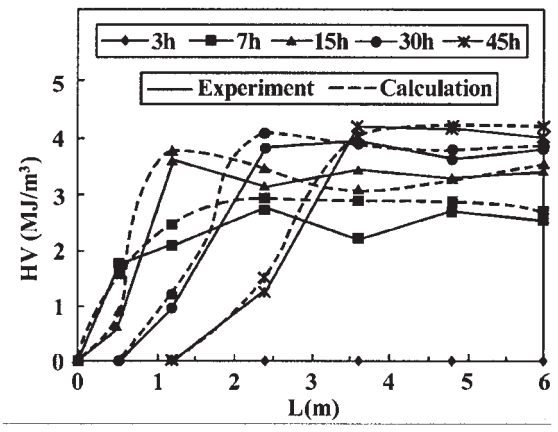

Figure 14. Experiment value and calculation value of the gas heat value at various times of gasification.

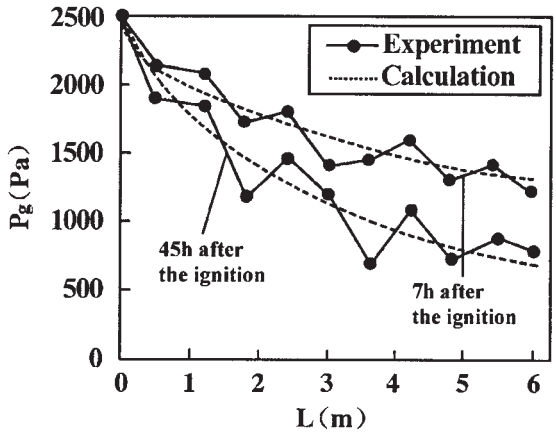

Figure 15. Pressure field in the gasification tunnel 7 h and 45 h after the ignition.

comparatively long gasification channel, due to the short period of time and the low temperature in the oven, the heating value of gas is comparatively low; 45 h after the ignition, the temperature of the oven increases. Although the length of the gasification channel is relatively short, the heating value of the outlet gas is higher than that of previous one. Therefore, maintaining an ideal temperature field and comparatively longer gasification channel is conducive to the stability and improvement of the heating value for the gas.

Figure 15 demonstrates that the simulated calculation values of the gas pressure basically conform with the measured ones. The relative error at the second time between calculated values and measured ones is 4.13%–12.69%, with the average drop rate of fluid pressure 6.01%. From Figure 15, we can know that, 45 h after the commencement of gasification, the error of the simulated calculation for pressure is 8.25%–17.47%, with the average drop rate of the gas pressure along the gasification channel 10.91%. It can be concluded that, with the prolonging of gasification time, the extent of drop for the fluid pressure rises and the calculation error increases. The major reasons are the following: at the very beginning of the experiment, the gas moves along the free gasification channel with little resistance on the fluid. The fluctuation for the curve of the experiment is small, so the drop rate and the calculation error are low, but the calculation value is comparatively high. With the development of the gasification process, the coal layers over the gasification channel, due to the effect of high temperature, expands, splinters and falls onto the gasification channel because of deadweight, which fills the bottom of the gasification channel with loose coal chunks. Thus, the free gasification channel transforms into a percolation-patterned one. The seepage movement of the gas will go on in the porous media. The resistance on the gas movement increases by a large margin, so does the extent of the pressure drop, which also tends to be stable. The curve between the experiment and calculation takes on a good conformity. Considering the changes in movement conditions, in the preliminary determination of major model parameters, such as the coefficient of conduction pressure, permeability, the involvement of personal or empirical factors in the consideration of relevant calculation coefficients results in a certain error in the initial parameters calculation, which causes oscillatory occurrence in the value of initial numerical simulation.

In short, the simulated results indicate the calculated values can conform with the measured values, which shows that the establishment of mathematical models on heat and mass transfer in the process of underground coal gasification, the determination of parameters, the analysis and treatment of boundary conditions and the solution method are correct. This will provide necessary theoretical evidence and scientific guidance for the further comprehensive quantitative study and production practice of underground coal gasification.

Conclusion

(1) According to the features of gasification process, on the basis of the model test, the nonlinear coupled mathematical models on the underground coal gasification for inclined coal layers are established. The simulated results demonstrate the calculated values can conform with the measured ones comparatively well, which proves that the numerical simulation on the temperature field, concentration field and pressure field is reasonable in the underground coal gasification under the experimental condition.

(2) The numerical simulation results show that, in high temperature zone, the calculated value of the temperature field is a bit bigger than the measured one; the change gradient of the measured value of the concentration for various compositions in the gas is bigger than that of the calculated value; temperature field has a great influence on the heating value of the gas. The heating value of the gas increases gradually with the prolonging of gasification time. The calculated value of heating value is basically the same with the experimental one. Apparently, the ideal temperature field is conducive to the improvement on the gas quality and the stability of the gasification process.

(3) According to the calculation results, the relative error between the calculation value and measurement one of the fluid pressure and its drop rate increases gradually with the process of gasification. The change of the flow condition in gasification channel is mainly responsible for the change of the calculation error.

(4) The numerical calculation results basically reflect the real patterns of variation for the temperature field, concentration field and pressure field in the underground coal gasification for the inclined coal seams, which will provide necessary scientific theoretical evidence for the further quantitative study on the underground coal gasification process and the predictions of its variation patterns.

Acknowledgments

This work was supported by the National Natural Science Foundation of China (Ratification No.: 59906014), and by the National Natural Science Foundation of China (Ratification No.: 50276066, 20207014). The technical contributions of Professor Yu Li and Dr. Wang Zaiquan are gratefully acknowledged by the author. The author also gratefully thanks Professor Xiang Youqian, Wang Jialian, and Gao Wenjun, for helpful discussion. Support received for this research from the Engineering Research Centre (ERC) for Clean Coal Technology of the China University of Mining and Technology (CUMT) is gratefully acknowledged.

Notation

a = coefficient in Eq. 3
a_m = coefficients in Eqs. 10–15 ($m = 1, 2, -2, -3, 3, -1$)
a_I = coefficients of difference equation (61) ($I = E, W, N, S$)

a_0 = parameter in Eq. 48, determined by $a_0 = \nu/g\bar{e}r_g$
a_c = the coefficient of conduction pressure, m^2/s
A_c = coefficient in Eqs. 1–4 and Eqs. 6–8
$\mathbf{A}$ = length vector of a certain interface for the grid, m
A_e = length of the e plane, m
$\mathbf{A}_e$ = length vector of the e plane, m
A_k = length of the k interface ($k = e, w, n, s$), m
A_i = coefficient of the expression (65), which varies with the kinds of substances
$A(|\bar{P}|)$ = form function
$A(|\bar{P}_k|)$ = form function of the k interface ($k = e, w, n, s$)
b = coefficient in Eq. 3
b_h = coefficients in Eqs. 10 and 11 ($h = 1, 2$)
b_C = constant term of difference Eq. 61
b_0 = parameter in Eq. 48, determined by $b_0 = \beta d/\overline{gner}_g$
$\bar{B}_i$ = coefficient of the expression (Eq. 65), which varies with the kinds of substances
C = overall mole concentration of gas, mol/m^3
C_e = convection (or flowing) intensity at the e plane in Figure 2
C_k = convection intensity
$\bar{C}_i$ = coefficient of the expression (Eq. 65), which varies with the kinds of substances
C_{gi} = specific heat of the composition i for the gas phase, J/kg K
C_S = the specific heat of solid phase, J/kg K
d = average compromising particle size, m
D = diffusion rate of every composition along the axial and radial direction, m^2/s
D_e = diffusion intensity at the e plane in Figure 2
$D_{eff,i}$ = effective diffusion coefficient of the composition i, m^2/s
D_k = diffusion intensity
D_K = diameter of the particle, m
e = interface between two grid points
$\bar{e}$ = permeability, μm^2
F = encompassed area of a control body, m^2
F_1 = area of heat radiation, m^2
F_S = specific surface area of the solid particle, m^2/m^3
F_ϕ = area of the grid, m^2
g = gravitational acceleration, m/s^2
H_i = enthalpy of formation for the gas composition i, J/mol
$\mathbf{J}$ = vector of total flux item
$\mathbf{J}_e$ = vector of general flux item at the e plane in Figure 2
K = rate constant
K_j = equilibrium constant of chemical reaction j
K_f = the equilibrium constant expressed in terms of the partial fugacity of every composition
L = length of gallery, m
m_i = mass flowing quantity of the composition i, kg/m^3
n = interface between two grid points
$n1$ = coefficient of the expression (Eq. 65)
$n2$ = coefficient of the expression (Eq. 65)
$\bar{n}$ = porosity
N_u = Nulet dimensionless number
$\bar{P}$ = Peclet number
P_i = partial pressure of composition i in the mixed gas, Pa
P_g = fluid pressure, Pa
P_k = ratio of the C_k and D_k
Q = quantity of heat transfer, W
Q_g = heat losses of the gas phase, J/m^3 s
Q_S = heat losses of solid phase, J/kg s
r = r-coordinate
r_0 = distance between boundary of the outer coal seam and x-coordinate axis, m
r_1 = radius of gallery, m
r_g = weight degree, N/m^3
R = universal gas constant, J/kmol K
RHT = quantity of heat exchange by radiation, W
R_j = chemical reaction rate, mol/m^3 s
R_K = radius of the particle, m
R_r = radius of the reaction core, m
s = interface between two grid points
S_C = constant relative to ϕ in Eq. 54
S_i = generating rate of the composition i in the chemical reaction, mol/m^3 s
SH = heat of formation for the gas phase, J
S_P = constant relative to ϕ in Eq. 54
S_ϕ = source item
t = time, s
T = temperature, K
T_0 = temperature of solid phase at the inlet of gallery, K
T_g = temperature of gas phase, K
T_{gb} = temperature of the gas at the inlet of the gallery, K
T_{gp} = temperature of the gas at wall plane boundary, K
T_{g0} = initial temperature of the gas at the inlet of the gallery, K
T_K = temperature of reaction core, K
T_{K1} = temperature of the solid particle, K
T_S = temperature of solid phase, K
T_{S0} = known temperature of the solid phase, K
$T_{S\infty}$ = temperature of the outer coal seam, K
u = velocity of the fluid, m/s
w = interface between two grid points
W_g = source-sink item
x = x-coordinate
y_i = mole fraction of the composition i
y_{i0} = mole fraction of gasification agent at the inlet of gallery

Greek letters

α = coefficient of heat convection, W/m^2 K
α_L = coefficient of heat convection through ash dreg layers, W/m^2 K
α_K = coefficient of heat convection through reduced film, W/m^2 K
α_S = coefficient of heat-exchange by radiation through reduced film, W/m^2 K
α'_S = coefficient of heat-exchange by radiation through ash dreg layers, W/m^2 K
γ_j = coefficient of weighing and measuring for the chemical reaction j
ε_S = radiation rate of solid phase, W/m^3 K^4
ε_g = radiation rate of gas phase, W/m^3 K^4
δ = thickness of the ash dreg layer, m
δ_0 = thickness of the reduced film, m
δ_k = distance between two grid points on the vertical k interface, m
δx = distance between two grid points, m
$\zeta_1(T)$ = function of the coefficient of heat conductivity, W/m K
$\zeta_2(T)$ = function of the coefficient of heat-exchange by radiation, W/m K
ν = coefficient of movement viscosity, m^2/s
β = coefficient of geometrical shape for the media particles
ϕ = dependent variable
Γ_e = exchange coefficient at the e plane in Figure 2, determined by Eq. 60
Γ_E = exchange coefficient at the grid point E in Figure 2
Γ_k = exchange coefficient at the k interface ($k = e, w, n, s$)
Γ_P = exchange coefficient at the grid point P in Figure 2
Γ_ϕ = coefficient of exchange corresponding to the variable ϕ
φ = characteristic variable of the control body
ϕ_I = variables of difference Eq. 61 ($I = E, W, N, S$)
ϕ^* = previous iterative value for the variable ϕ
ΔE_j = activation energy of chemical reaction j, J/mol
ΔG = free enthalpy of standard formation, J/mol
ΔH_j = reaction heat of the chemical reaction j, J/mol
Δt = time step size, s
σ = Stefan-Baltzmann constant, W/m^2 K^4
ε_q = coefficient of heat radiation
λ_g = coefficient of heat conductivity for the gas phase, W/m K
λ_S = coefficient of heat conductivity for the solid phase, W/m K
ρ = fluid density, kg/m^3
ρ_g = density of the mixed gas, kg/m^3
ρ_{P^0} = fluid density of the point P at the previous time, kg/m^3
ρ_S = density of solid phase, kg/m^3
$[[\ ]]$ = selecting the maximum in the square brackets
∇ = Hamilton operator

Subscripts

b = boundary
c = coefficient
C = constant
eff = effective
f = partial fugacity

g = gas
i = composition i
j = chemical reaction j
k = k interface
p = wall plane
P = grid point P
P^0 = state of the point P at the previous time
q = heat radiation
r = radius
S = solid
ϕ = variable
∞ = outer coal seam
0 = known value

Literature Cited

1. Yang LH. Study on the seepage combustion method in underground coal gasification. 2nd ed. Xuzhou: China University of Mining & Technology Press; 2004.
2. Yang LH, Song QY, Li YJ. Underground coal gasification project (1st ed). Xuzhou: China University of Mining & Technology Press; 2001.
3. Liang J. Study on the stability and controlling technology of underground gasification in steep coal seam (Dissertation), China University of Mining and Technology; 1997.
4. Liu SQ, Liang J, Yu L. Reaction character and influence factors of CO_2 in underground coal gasification. J of China University of Mining & Technology. 2000;29:606–609.
5. Debelle B, Malmendier M. Modeling of flow at Thulin underground coal gasification experiments. *Fuel.* 1992;71:95–104.
6. Martin JM, Layne AW, Siriwardane HJ. Thermo-mechanical modeling of ground movements associated with large underground coal gasification cavities in thin coal seams. Proc. 10th UCG Symp., Fallen Leaf Lake, California; (April)1984;295–307.
7. Крейнин ЕБ. Two-stage underground coal gasification. *Coal Chemical Industry.* 1993;6:61–63.
8. Куктешов ВМ. Increasing efficiency of underground coal gasification. Collections of Translated Works on Mining Technology. 1988; 9:17–19.
9. Gunterman K. The comprehensive experimental model and mathematical model on the underground coal gasification. Collections of Translated Works on Mining Technology. 1988;9:6–10.
10. William BK, Robert DG. Underground coal gasification: the state of the art. 1st ed. New York: Am In Ch Eng; 1983.
11. Dufaux A. Modeling of the UCG process at Thulin on the basis of thermodynamic equilibriums and isotopic measurements. *Fuel.* 1990; 69:624–632.
12. Advani SH, Lee JK, Chen KS. Geomechanical modeling associated with underground coal gasification process. Proceedings of the Twelfth Annual Underground Coal Gasification Symposium, Washington, DC, (August)1986;272–278.
13. Guntrmann K, Gudenau HW, Franke FH. "An integrated UCG-simulation model of laboratory work and mathematical modeling. Proceedings of the Twelfth Annual Underground Coal Gasification Symposium," Washington, DC, (August)1986;207–216.
14. Yeary D, Riggs JB. Experimental study of lateral cavity growth mechanisms. Proceedings of the Twelfth Annual Underground Coal Gasification Symposium. Washington, DC, (August)1986; pp158–164.
15. Yu F. The structural dynamic simulation on underground coal gasification. Collections of Translated Works on Mining Technology. 1992; 13:1–3.
16. Liu SQ, Liu JH, Yu L. Environmental benefits of underground coal gasification. J of Environ Sci. 2001;9:51–54.
17. Liu BY, Qiu P. Study on the underground coal gasification technology. *Clean Coal Technol.* 2003;9:23–29.
18. Guo CW. A review of the study on mathematical models on underground coal gasification. *Mining World.* 1994;15:2–5.
19. Liu SQ, Liang J, Yu L. Study on the abatement technology of CO_2 discharged from UCG. *Proceedings of the Second International Symposium on Clean Coal Technology.* Beijing, 1999;541–545.
20. Liu SQ, Liang J, Chang J, Yang Z, Yu L. UCG model test of Huating coal with oxygen-steam as gasification agent. *J of Southeast University (Natural Science Edition).* 2003;33:355–358.
21. Liu SQ. Study on the regularity of CO_2 production in the process of underground coal gasification and on the disposal method of CO_2 (Dissertation). China University of Mining & Technology; 2000;73–76.
22. Guo CW. Study on long-tunnel large-section two-stage underground coal gasification (Dissertation). China University of Mining & Technology; 1993; pp109–114.
23. Xiang YQ. Mathematical model, modeling calculation and optimal operation for coal gasification. *Coal Conversion.* 2002;25:60–64.
24. Wu RY. Coal gasification. 1st ed. Xuzhou: China University of Mining & Technology Press; 1988.
25. Yang LH. Numerical simulation on non-steady state temperature field in the underground coal gasification. J of China University of Mining & Technology. 2000;29;140–143.
26. Fan WC, Wan YP. The model and calculation of flowing and combustion (2nd edition). Hefei: China University of Science & Technology Press; 1992.
27. Zhou LX. Combustion theory and chemical fluid mechanics. 1st ed. Beijing: Science Press; 1986.
28. Qin KF, Fan JK. Combustion fluid mechanics. 1st ed. Beijing: Hydroelectricity Power Press; 1991.
29. Gao J R. Momentum, heat, and mass transmission principle. 1st ed. Chongqing: Chongqing University Press; 1987.
30. Chen CK. Computation fluid mechanics. 2nd ed. Chongqin: Chongqing Press; 1992.
31. Xiang YQ, Hedden K. The determination of dynamic data for solid fuel in the process of conversion. *Gas & Heat.* 1986;6:4–11.
32. Ruprecht P. A computer model of entrained coal gasification. *Fuel.* 1988;67:739–742.
33. Fu WB, Zhang YL, Wang DA. Combustion science. 1st ed. Beijing: Higher Education Press; 1989.
34. Zhao JX., Yi Y. Numerical and experimental study on the turbulence combustion model. *J of Engg Thermophysics.* 1994;15:99–104.
35. Tao WQ. The progress of calculation heat transfer in modern times 1st ed. Beijing: Science Press; 2000.
36. Bu XM, Peng WW, Xiang YQ. The study of the mathematical models on the pressurization gasification in fixed beds. *Coal Chemical Industry.* 1993;17:6–15.

Manuscript received Jun. 8, 2004, and revision received Feb. 14, 2005.